

# Bamboo: Building Mega-Scale Vision Dataset Continually with Human-Machine Synergy

Yuanhan Zhang<sup>1</sup> Qinghong Sun<sup>2</sup> Yichun Zhou<sup>3</sup> Zexin He<sup>3</sup>  
Zhenfei Yin<sup>4</sup> Kun Wang<sup>4</sup> Lu Sheng<sup>3</sup> Yu Qiao<sup>5</sup> Jing Shao<sup>4</sup> Ziwei Liu<sup>1</sup>

<sup>1</sup>S-Lab, Nanyang Technological University

<sup>2</sup>Beijing University of Posts and Telecommunication <sup>3</sup>Beihang University

<sup>4</sup>SenseTime Research <sup>5</sup>Shanghai AI Laboratory

{yuanhan002, ziwei.liu}@ntu.edu.sg

sunqinghong@bupt.edu.cn

{buaazyc, jacquesdeh, lsheng}@buaa.edu.cn

{yinzenfei, wangkun, shaojing}@sensetime.com

qiaoyu@pjlab.org.cn

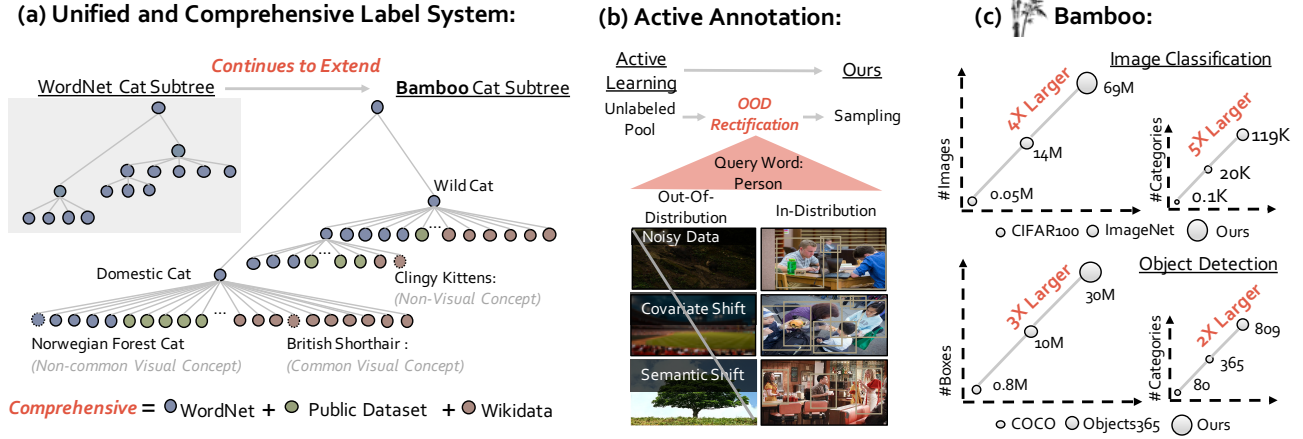


Figure 1. **The overview of Bamboo Dataset.** Bamboo is a new mega-scale vision dataset built on a comprehensive label system with human-machine synergy. (a) Our label system BambooTX continually extends from WordNet with our solutions. Concepts in the label system are distinguished as “common visual”, “non-common visual” or “non-visual” concepts. (b) Raw data crawled by the query word *person* includes both the in-distribution (ID) data and out-of-distribution (OOD) data. OOD data implies noisy data, covariate shift data and semantic shift data. Noisy data presents none of the object in it. covariate shift data implies person semantic. However, people in it are too small for annotators to label. Semantic shift data presents another semantic object (tree). *OOD rectification* mitigates the ineffectiveness of modern active learning in realistic scenarios through filtering this OOD data. (c) Bamboo actively collects 69M classification annotation and 28M object bounding box annotations.

## Abstract

Large-scale datasets play a vital role in computer vision. Existing datasets are either collected according to heuristic label systems or annotated blindly without differentiation to samples, making them inefficient and unscalable. How to systematically collect, annotate and build a mega-scale dataset remains an open question. In this work, we advocate building a high-quality vision dataset actively and continually on a comprehensive label system. Specifically, we

contribute **Bamboo Dataset**, a mega-scale and information-dense dataset for both classification and detection. It is built upon this human-machine synergy with two appealing properties: **1) Label System:** we integrate categories from 24 public datasets and collect 170,586 new categories from knowledge bases, forming a hierarchical label system with 304,048 categories. The label system is easily extendable under our designed hierarchy, and its concepts are further distinguished as “visual” or “non-visual”. **2) Active Annotation:** based on a real-world data pool of 370M raw

images crawled by the label system, only informative samples are selected for manual labeling through our human-machine active annotation framework. We find that rectifying out-of-distribution samples is crucial for active learning to function in realistic scenarios. Bamboo aims to populate these comprehensive categories with 69M image classification annotations and 28M object bounding box annotations. Compared to ImageNet22K and Objects365, models pre-trained on Bamboo achieve superior performance among various downstream tasks (6.2% gains on classification and 2.1% gains on detection). In addition, we provide valuable observations regarding large-scale pre-training from over 1,000 experiments. Due to its scalable nature on both label system and annotation pipeline, Bamboo will continue to grow and benefit from the collective efforts of the community, which we hope would pave the way for more general vision models. Bamboo is available at <https://github.com/Davidzhangyuanhan/Bamboo>.

## 1. Introduction

Large-scale pre-trained models, either trained in a supervised [26, 38, 78] or unsupervised [10, 14, 30] manner, have become a foundation for modern computer vision. Various applications are enabled by transferring the pre-trained models (e.g. ImageNet or COCO pre-trained models) to downstream tasks. Most importantly, the fuel of these foundation models [6] relies on the availability of increasingly large and diverse datasets [18, 41, 46, 66].

Building a high-quality dataset requires careful considerations in selecting both the label and data. However, existing datasets are either collected according to ad-hoc label systems or annotated blindly with no differentiation to samples, making them inefficient and unscalable. For example, ImageNet [18] uses the WordNet [50] as its label system. Nevertheless, not only the limited number of concepts in WordNet prevents ImageNet from covering a complete spectrum of concepts in the natural domain, but also the non-visual words, e.g. vitamin, in WordNet leads to ImageNet to annotate words that could be non-suitable for computer vision tasks. In addition, it is extremely inefficient for ImageNet to randomly select images from the unlabeled pool to annotate.

In this work, we systematically investigate how to build a mega-scale dataset in an active and continual manner. Motivated by the above-mentioned limitation of the construction of the existing dataset, we design the following two philosophies in terms of label and data as key ingredients:

**1) Unified and Comprehensive Label System.** A comprehensive label system is the cornerstone of building a mega-scale dataset. We form a unified label system with a hierarchical structure, consisting of 304,048 categories. It integrates label systems from 19 latest public image classification

datasets and five object detection datasets, and also absorbs 170,586 new categories from knowledge bases, e.g. Wikidata [73]. Beyond that, we conduct visibility tagging for all concepts and only keep 119,035 visual concepts for the subsequent candidate data collection.

**2) Active Data Annotation Pipeline.** Randomly selecting images from unlabeled pool to annotate is inefficient, but this problem is largely overlooked in existing dataset construction [18, 42]. Recently, researchers have been exploring active learning (AL) algorithms [17, 57, 63] to select the most informative samples for labeling. However, these methods typically fall short in the presence of out-of-distribution (OOD) data, due to their inaccurate uncertainty estimation under realistic scenarios. Therefore, we propose a new active data annotation pipeline by integrating *OOD Rectification* that is able to perform effective sample selection from massive data pool in the wild.

Building upon this human-machine synergy, we contribute **Bamboo Dataset**, a mega-scale and information-dense dataset for the pre-training of both classification and detection. Bamboo has three appealing properties:

- **Comprehensive.** It consists of 69M image classification annotations and 28M object bounding box annotations, spanning over 119K visual categories. The scale of the label system and the annotated data are the largest among all the publicly available datasets. We illustrate the comparison of Bamboo and publicly available datasets in the Fig 1 (c).
- **Information-Dense.** The label system and the annotated data are designed to guarantee both the coverage and informativeness. The label system is constructed by a thorough integration of public datasets and knowledge bases. The annotated data are specifically selected by our active annotation pipeline to reduce model uncertainty.
- **Continual.** Our label system enables the dataset to keep on growing with the automatic concept linking strategies. We can constantly absorb new categories in the real world and integrate them into our label system. Moreover, by leveraging the ever-increasing internet data, our active annotation pipeline will steadily expand the Bamboo dataset size in a sustainable manner.

Extensive experiments demonstrate that Bamboo dataset is an effective pre-training source. The Bamboo pre-trained model significantly outperforms CLIP ViT B/16 [55] pre-trained model with 6.2% gain (85.6% vs 91.8%) on classification, and outperforms Objects365 [64] pre-trained model with 2.1% gain (14.7% vs 12.6%) on CityPersons [86]. In addition, we provide valuable observations regarding large-scale pre-training from over 1,000 experiments. We hope the Bamboo dataset and these observations would pave the

way for the development of more general and effective vision models.

## 2. Related Work

**Learning of Representation at Scale.** Representation learning has advanced thanks to improvements in various learning paradigms and large-scale datasets. Supervised learning models [15, 31] leverage label information to supervise representation learning, achieving excellent performance among various downstream tasks. To avoid the need for annotations that require a tremendous amount of human and labeling cost, weakly-supervised and self-supervised pre-training methods have been proposed. Self-supervised methods [9, 10, 13, 19, 30, 43, 44, 51, 75, 85] with contrastive learning have shown that unsupervised pre-training produces features surpassing the supervised feature representations on many downstream tasks [40, 41, 52, 53, 76]. Large weakly-supervised datasets, such as Instagram hashtags [48] and JFT [66], helps model [77, 78, 88] achieve significant gains on downstream tasks. In addition, CLIP [55] pre-train models on both the image signal and text signal, achieving good performance for the zero-shot evaluation. Our study is part of a larger body of work on training models on sizeable supervised image datasets. As the labeling cost that hurdles the supervised learning dataset is becoming increasingly significant, we systematically investigate how to collect, annotate and build a mega-scale dataset efficiently, actively and continually.

**Active Learning.** Active learning (AL) aims at finding the minimum number of labeled images to have a supervised learning algorithm reach a certain performance [25, 27, 34, 35, 63, 67, 70, 72, 83]. The main component in an active learning loop is sampling strategies. The existing AL research is conducted on the curated datasets. Each data point in the labeled and unlabeled pool of these datasets is valid, *i.e.* available for labeling. However, curated datasets can hardly imitate the annotation in realistic scenarios where out-of-distribution data that is unavailable for labeling appears on a large scale in the unlabeled pool. From our experiments, we find the existing AL methods lag in realistic scenarios. Therefore, we propose a novel active annotation pipeline to improve the performance of AL methods in realistic scenarios.

## 3. Comprehensive Label System - BambooTX

A comprehensive label system is essential to building the mega-scale dataset. Starting from WordNet [50], we enrich its concepts from another two concept resource (Sec. 3.1) through four designed linking strategies (Sec. 3.2), building our comprehensive label system, namely Bamboo Taxonomy (**BambooTX**). With these linking strategies, BambooTX will continue to grow as we constantly absorb

new categories in the real world. Beyond that, all the concepts in our BambooTX are thoroughly tagged w.r.t. visuality and commonality (Sec. 3.3).

### 3.1. Concepts Resources

**WordNet.** WordNet is a lexical database of semantic relations between concepts in more than 200 languages. Each meaningful concept in WordNet, possibly described by multiple words or word phrases, is called a “synset”. Referring to ImageNet22K [18], we only use the Noun words of WordNet. WordNet is the foundation of our label system.

**Public Datasets.** We collect 24 public datasets, including ImageNet22K [18], OpenImages [42], COCO [46], iNaturalist [71], and *etc.*<sup>1</sup> These datasets cover a wide range of datasets in both image classification and object detection.

**Wikidata.** Wikidata [73] contains a large number of concepts, such as different kinds of foods, animals, and locations. As the number of concepts in Wikidata continues to grow, so far we have included 170,586 concepts from it. These concepts are the leaf nodes in their taxonomy.

### 3.2. Concepts Integration

With “string matching”, we can easily integrate the majority of concepts in Sec. 3.1. However, many categories cannot be integrated in WordNet in this way, *e.g.* *Airplane Cabin* from Places [87]. Therefore, we propose four parallel solutions to integrate these categories into WordNet. Specially, BambooTX continues to grow with these solutions as new categories steadily increase.

**Solution 1: Finding Common Name.** We leverage the Wikipedia Python library (<https://github.com/goldsmith/Wikipedia>) to query the common name for categories which are scientific name, *e.g.*, “Aves” is the scientific name for “birds”. If this common name belongs to WordNet, we extend the synset by adding this querying scientific name category.

**Solution 2: Leveraging on the subclassOf.** The taxonomy of Wikidata is contributed by adding the “subclassOf” that is related to the hypernyms relationship in the taxonomy of WordNet. Referred to [68], we link Wikidata leaf node concepts to the WordNet through leveraging on the “subclassOf”.

**Solution 3: Parsing the Concept.** Referred to the previous work [22], we can also link the concept to the WordNet through word parsing. For example, for the concept *Sumatran Orangutan*, we parse this concept [32] and get its head compound “Orangutan”. In this way, we add *Sumatran Orangutan* as the new hyponym of the “Orangutan” if “Orangutan” exists in WordNet.

**Solution 4: Linking to the Closed Synset.** We calculate the word embedding of both the synsets and given concepts

<sup>1</sup>The complete list of public datasets is reported in *Supplementary Material*.

through Spacy [32]. If a given concept cannot be linked to WordNet, we add this category to the hyponym of its nearest cosine distance synset.

### 3.3. Concepts Tagging

**Visuality.** Yang *et al.* has mentioned the non-visual category problem in their work [80]. While Yang *et al.* conduct visual concept tagging for *person* sub-tree of ImageNet based on crowd sourcing, their tagging has several drawbacks. Firstly, “The ease to arouse imagery (imageability)” and “the ease to characterize using images (visuality)” could be a mismatch. For example, *daughter* and *sister* have high image imageability scores, but lack visual cues other than being female. Secondly, annotators tend to assign low imageability scores to the unfamiliar concept. However, the unfamiliar concept can also be a visual concept. To mitigate the aforementioned problems, our concept tagging provides sample images, as shown in Fig. 4, to help the annotator understand the concept. A concept is considered as a non-visual concept if its sample images fall into one of these two criteria: 1) sample images do not infer common semantic information 2) the common semantic information of these sample images does not uniquely determine this concept. As shown in Fig. 2 (b), *Vitamin* does not share any common semantic information. *Economists* implies common semantic information, *i.e.* Man, but economists are not necessarily men.

**Commonality.** Based on the visual concepts, we further conduct common concept annotation for all visual concepts. Referred to [46], common concepts frequently occur in realistic scenes. Specifically, five annotators are asked to vote on each candidate concept. A concept is considered positive only if it receives at least three-fifths of the votes. Based on the proposed annotation method, we retain 809 common concepts for the annotation of object detection.

## 4. Active Dataset Construction - Bamboo

Equipped with the unified and comprehensive BambooTX, in this section, we start to actively construct dataset Bamboo. Our dataset construction consists of three main steps: 1) inheriting public datasets. (Sec. 4.1) 2) obtaining raw images from the Flickr.<sup>2</sup> (Sec. 4.2) 3) conducting an active annotation loop. By leveraging the ever-increasing internet data, our active annotation construction steadily expands the Bamboo dataset size in a sustainable manner. (Sec. 4.3)

### 4.1. Inheriting Public Datasets

As mentioned in Sec. 3.1, we use 24 datasets as concept resources, including 19 image classification datasets and 5 object detection datasets. Referred to the evaluation suite

<sup>2</sup><https://www.flickr.com/>.

---

### Algorithm 1: Outline of AL Framework

---

**input** : Raw unlabeled pool  $\Theta$ ; Number of active learning rounds  $T$ ; Neural network  $\phi$ ;

- 1  $\mathcal{P}^L(0) \leftarrow$  Annotating a few data from  $\Theta$  and adding all inherited data;
- 2  $\mathcal{P}^U(0) \leftarrow \Theta - \mathcal{P}^L(0) \cap \Theta$ ;
- 3 Initializing model  $\phi(0)$  based on  $\mathcal{P}^L(0)$ ;
- 4 **for**  $r \leftarrow 1$  **to**  $T$  **do**
- 5      $\mathcal{P}^R(r) \leftarrow$  Rectifying  $\mathcal{P}^U(r-1)$  w/  $\phi(r-1)$ ;
- 6      $\mathcal{S}^U(r) \leftarrow$  Sampling in  $\mathcal{P}^R(r)$  w/  $\phi(r-1)$ ;
- 7      $\mathcal{S}^L(r) \leftarrow$  Annotating valid data from  $\mathcal{S}^U(r)$ ;
- 8      $\mathcal{P}^U(r) \leftarrow \mathcal{P}^U(r-1) - \mathcal{S}^U(r)$ ;
- 9      $\mathcal{P}^L(r) \leftarrow \mathcal{P}^L(r-1) \cup \mathcal{S}^L(r)$ ;
- 10    Training  $\phi(r)$  on  $\mathcal{P}^L(r)$ ;
- 11 **end**

---

of popular transfer learning study [30, 39, 84], we select 12 datasets for downstream evaluation, and inherit the annotation of the other 12 datasets into Bamboo, *i.e.* 10 image classification datasets and 2 object detection datasets. In total, we inherit 27,848,477 classification annotations and 21,983,223 object bounding box annotations from those 12 datasets.

### 4.2. Obtaining Raw Data

By searching query words from Flickr, we collect raw data, forming the raw unlabeled pool  $\Theta$ . For image classification, one query word has one visual concept mentioned in Sec. 3.3. For object detection, one query has two concepts, *i.e.*, common concept + scene semantic word or common concept + common concept. For example, *dog + street* or *dog + ball*. To further enrich the searching results, any given query word can be converted to its synonyms or its Chinese, Spanish, Dutch and Italian version for querying. Totally, we obtain a 170M unlabeled pool for classification and a 200M unlabeled pool for detection.

### 4.3. Active Annotation Loop

In this section, we describe our active annotation framework that can be applied for realistic scenarios. The outline of our active learning (AL) framework is shown in Algorithm 1. We start from a network  $\phi(0)$  trained on the initial labeled data pool  $\mathcal{P}^L(0)$  and then proceed with the active annotation loop. At the first step in each round  $r$ , the current AL algorithms directly mine the most informative sample set  $\mathcal{S}^U(r)$  from the latest unlabeled pool  $\mathcal{P}^U(r)$ . These informative samples are usually the most uncertain samples for the model. Nonetheless, in realistic scenarios, those uncertain samples can imply both the samples in-distribution and the samples out-of-distribution shift (OOD data). As



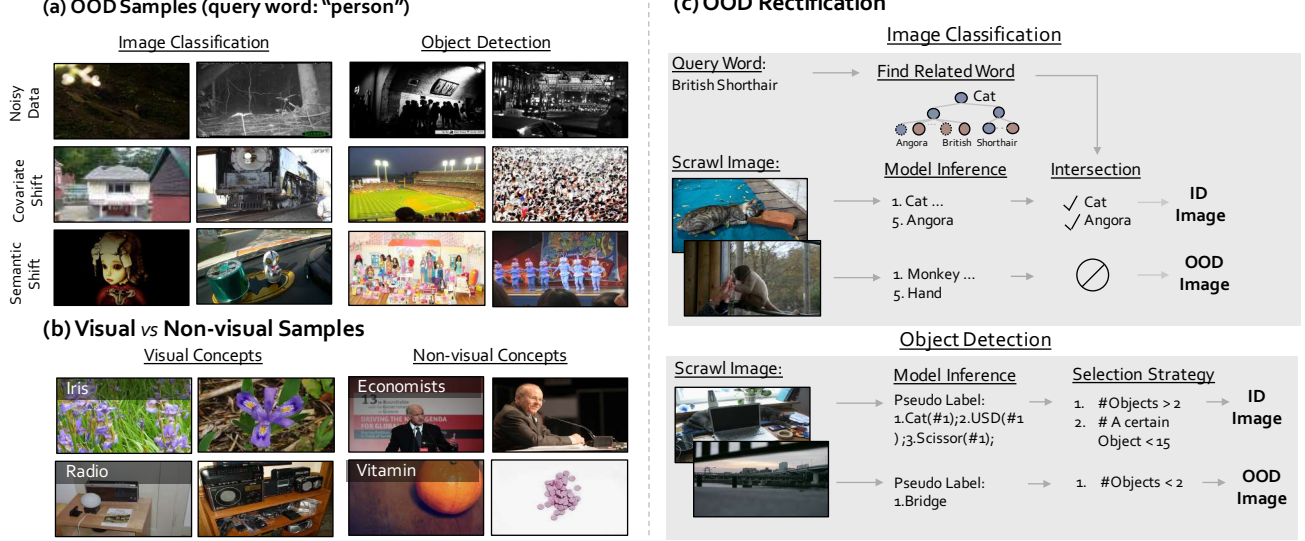


Figure 2. (a) The illustration of out-of-distribution (OOD) data in realistic scenarios. Mainly, three types of OOD data exist in the unlabeled data pool, including noisy data, covariate shift data (*i.e.*, OOD samples from a different domain), and semantic shift data (*i.e.*, OOD samples are drawn from different classes). (b) The illustration of Non-visual Concepts. *Vitamin* do not share any common semantic information. *Economists* implies common semantic information, *i.e.* Man, but economists are not necessarily men. (c) The illustration of OOD rectification. OOD rectification filters OOD data in the unlabeled data pool, which is crucial for active learning.

shown in Fig. 2 (a), the OOD data includes noisy data, semantic shift data (*e.g.*, samples are drawn from different classes), and covariate shift data (*e.g.*, samples from a different domain) [79]. This data is “invalid data” for annotators because it can hardly infer the accurate visual cues of the related concepts. Without the cleaning of  $\mathcal{P}^U(r)$ , such “invalid data” holds a great proportion of  $\mathcal{S}^U(r)$ . What’s worse, AL algorithms prefer to select much more “invalid data” from  $\mathcal{P}^U(r)$  than random sampling, resulting in lower efficiency, as mentioned in Sec. 6.2. Hence, in our active annotation loop, the first step in each round  $r$  is the OOD rectification. This step works for filtering out the OOD data from  $\mathcal{P}^U(r)$ . After this step, we retain a rectified data pool  $\mathcal{P}^R(r)$  for the sampling. During sampling, a batch of images  $\mathcal{S}^U(r)$  is selected for labeling, making use of the computed informativeness score but also encouraging diversity in the selected batch. Finally, annotators label the “valid data” in  $\mathcal{S}^U(r)$ , forming  $\mathcal{S}^L(r)$ . Next, we describe our active annotation loop in detail, consisting of an initialization step, an OOD rectification step, a sampling step, and an annotation step.

#### 4.3.1 Model Training.

In the initial round ( $r = 0$ ), we construct  $\mathcal{P}^L(0)$  to initialize the model  $\phi(0)$ .  $\mathcal{P}^L(0)$  includes the inherited data and the new annotated data. The new annotated data is built based on the concepts that are not included in the inherited dataset. Specifically, we annotate 50-100 images/instances for each of these concepts. The subsequent round  $r$  ends

with training a new model  $\phi(r)$  based on  $\mathcal{P}^L(r)$ .

#### 4.3.2 OOD Rectification.

1) Image Classification. In this step, we rectify the latest unlabeled data pool  $\mathcal{P}_C^U(r-1)$ . As shown in Fig 2 (c), in each round  $r$ , we firstly utilize  $\phi_C(r-1)$  trained on  $\mathcal{P}_C^L(r-1)$  to acquire predictions of each image in  $\mathcal{P}_C^U(r-1)$ . We infer an image is out-of-distribution if its top-5 predicted categories do not overlap with its related categories. Specifically, we define the related categories of an image as the sub-population of hypernyms of its query word. If an image is not out-of-distribution, we add it into  $\mathcal{P}_C^R(r)$  for the further data sampling. In Sec. 6.2, we empirically observe that OOD rectification is essential for AL to function in realistic scenarios.

2) Object Detection. Similar to classification, we acquire proposal predictions of each image in  $\mathcal{P}_D^U(r-1)$  by  $\phi_D(r-1)$ . On the one hand, we filter out the image with less than two proposals, such image might be noisy data or semantic shift data. On the other hand, we filter out the image that has more than 15 identical semantic proposals, since such image might be the covariate shift data. As shown in Fig 2 (c), the remaining data forms  $\mathcal{P}_D^R(r)$  for the data sampling.

#### 4.3.3 Active Sampling.

In this step, the goal is to select a batch of samples (5M for classification, 100K for detection)  $\mathcal{S}^U(r)$  from the latest rectified data pool  $\mathcal{P}^R(r)$  for annotation. In Sec. 6.2,

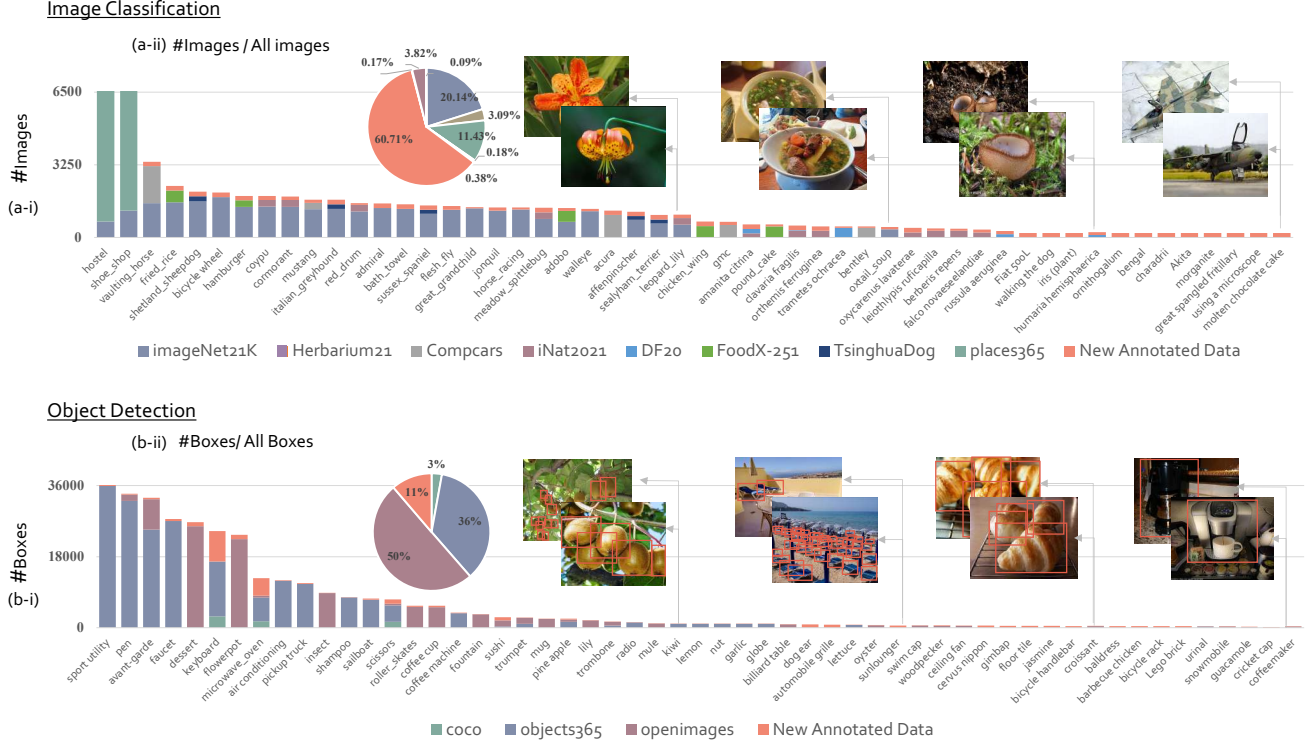
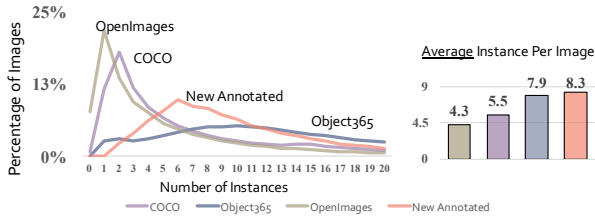


Figure 3. **Sorted distribution of image number per category in the Bamboo.** (a-i) Bamboo-CLS contains 68,884,828 images spread across 119,035 categories. Category names are shown for every 250 intervals. Bamboo-CLS includes some fine-grained concepts that not be included in the current public datasets, such as *Folland Midge*. (a-ii) The new classification annotated data accounts for 43.2% of images in Bamboo. (b-i) Bamboo-DET contains 3,104,012 images across 809 categories. Category names are shown for every 16 intervals. (b-ii) The new detection annotated data accounts for 11% of images in Bamboo.

Table 1. **Left: The statistics of the number of bounding boxes per image.** Quantitatively, our new annotated data has 8.3 instances (on average) per image, which is more dense compared with the other datasets like COCO and OpenImages. **Right: Summary of Bamboo.** Bamboo is the largest fully annotated vision dataset available to the general research community, in terms of the total number of images, the number of concepts, and the number of bounding boxes (for object detection task).



Datasets	Concepts	Images	Boxes	Anno.
YFCC-100M [69]	-	100M	-	No
ImageNet22K [18]	22K	14M	-	Yes
<b>Bamboo-CLS</b>	<b>119K</b>	<b>69M</b>	-	Yes
COCO [46]	80	118K	1M	Yes
Objects365 [64]	365	609K	10M	Yes
OpenImages [42]	600	2M	14M	Partial
<b>Bamboo-DET</b>	<b>809</b>	<b>3M</b>	<b>27M</b>	Yes

we compare various AL methods in our simulated realistic scenarios. In both classification and detection tasks, after the OOD rectification, AL methods (ClusterMargin [17] and Core-Set [62]) that consider both the uncertainty and diversity, select the most valuable data for model training.

#### 4.3.4 Human Annotation

We describe and visualize our human annotation interface for concepts tagging and image annotation, which works for image classification and object detection tasks. We pro-

vide hyperlinks for previewing the reference images instead of crawling these images directly, avoiding the impact of image copyright infringement.

#### 4.4. Concepts Tagging

As is discussed in Sec. 2.3 of the main paper, we conduct concepts tagging in the aspects of visually and commonality. Fig. 4 (a) and (b) show our user interface for visually tagging and commonality tagging, respectively. We design the labeling task by asking the annotator to answer yes or no. Annotators answer this question according to the meta-

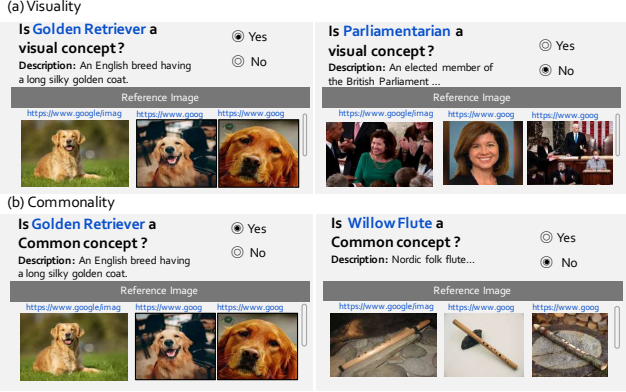


Figure 4. **User interfaces for concept tagging.** The meta information of the concept is presented on the interface consisting of tag, description, and reference images. (a) Interface for filtering out non-visual concepts. (b) Interface for selecting common concepts which frequently occur in realistic scenes.

information of the concept presented on the interface consisting of tag, description, and reference images.

#### 4.5. Image Annotation

**Image Classification.** Fig. 5 (a) shows our user interface for image classification task. Like the interface for concept tagging, the meta information of each concept consists of a tag, description, and reference images. As discussed in Sec. 3.3.4 of the main paper, annotators are paid for determining whether the unlabeled image conforms to the concept. The yes option will be marked if the annotator provides a positive answer to the question above.

**Object Detection.** Unlike the image classification task, a single unlabeled image for object detection typically has multiple pseudo labels. Especially, as shown in Fig. 5 (b), due to this unlabeled image having four pseudo labels, *i.e.*, person, bag, car, wheel, it is assigned to four annotators. As mentioned in Sec. 3.3.4 of the main paper, each annotator is responsible for annotating a specific category. Like the interface for concept tagging, the meta information of each concept consists of a tag, description, and reference images.

Before bounding box labeling, the annotator needs to determine the legality of the image. If the unlabeled images contain pornography or violent content, annotators should click the Invalid Image button to filter them out. Besides, annotators should regard noisy data or semantic shift data as invalid data. The purpose of Group bbox option is identical to GroupOf in OpenImages [42]. The box that covers more than five bounding boxes of the same category, which heavily occlude each other, should be marked as Group bbox. Other clear bounding box are supposed to be marked as Normal bbox option.

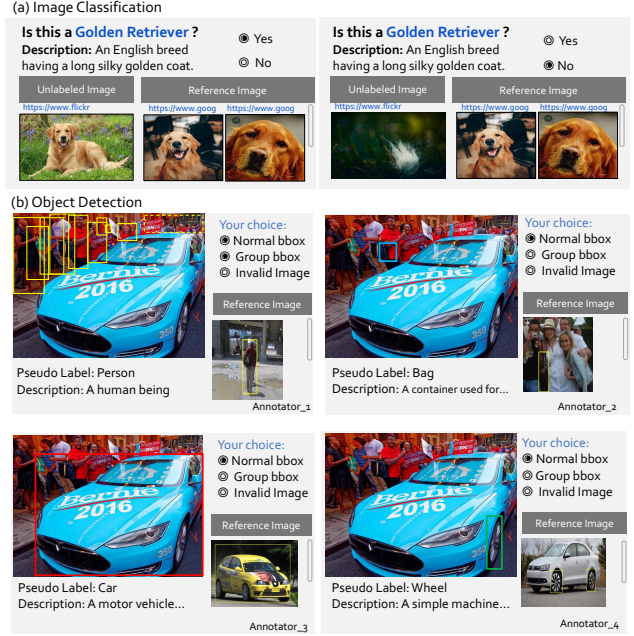


Figure 5. **User interfaces for image annotation.** (a) Interface for the image classification task. (b) Annotation procedure for the object detection task. The image is assigned to different annotators based on its multiple pseudo labels. Before bbox labeling, the annotator needs to determine the legality of the image. As for the valid images, the annotator needs to mark the bboxes with the normal option or group option. The criteria for the bbox attribute option are described in detail in Sec. 4.5.

#### 5. Dataset Statistics

**Image Classification (Bamboo-CLS).** Bamboo-CLS has 68,884,828 images spread across 119,035 categories. Specifically, 42,648,217 out of 68,884,828 images are newly annotated, which is twice of ImageNet22K. In addition, 20,000 out of 119,035 categories are from Wikidata. These categories mainly are fine-grained concepts, such as *Folland Midge* (one type of fighter) and *hemaria hemishphaerica* (a species of fungi). To our knowledge, Bamboo-CLS is the largest clean image dataset available to the vision research community, in terms of both the total number of images and the number of categories that have been fully annotated.

**Object Detection (Bamboo-DET).** Bamboo-DET has 3,104,012 images across 809 categories. Specifically, 557,457 images are newly annotated and 150 concepts are from the Wikidata.

As shown in Fig. 3, we illustrate the sorted distribution of image number per category in the Bamboo. In addition, we provide the statistics on instances per image of Bamboo-DET. As shown in Table 1, Our newly annotated data has 8.3 instances (on average) per image, which is dense than existing datasets, *i.e.* MS-COCO, Object-365 and OpenIm-



ages. We carefully discuss the potential legal issue of Bamboo, *e.g.* the copyright and privacy issue, and the data overlapping issue, in the *supplementary material*.

## 6. Experiments

### 6.1. Experimental Setups

**Datasets.** In the following sections, we adopt the downstream datasets that are widely used in the transfer learning study [30, 39, 84]. For models pre-trained on the image classification datasets, we use CIFAR10 [41], CIFAR100 [41], OxfordFlower [52], Food101 [7], Caltech101 [23], OxfordPets [53], DTD [16], StanfordCars [40], FGVC-Aircraft [49], SUN397 [76], ImageNet1K [60] as the downstream evaluation datasets. As for the object detection task, we select PASCAL VOC [21] and CityPersons [86] as the downstream evaluation datasets. These datasets cover a wide range of image domains. The number of images in each dataset ranges from 2,000 to 80,000, and the number of classes in each dataset ranges from 10 to 8,000.

**Evaluation Protocol.** For the classification task, we use image features taken from the penultimate layer of each model, ignoring any classification layer provided. We train a logistic regression classifier for the linear probe evaluation setting. For the detection task, we finetune the entire model loaded with its backbone and FPN weights. We only report the evaluation performance of models on downstream datasets.

### 6.2. Studies on Active Annotation

In existing active learning (AL) works [17, 33], researchers conduct experiments on the curated dataset where all the leave-out unlabeled data are “valid” data and can be labeled. However, in realistic annotation scenarios, the unlabeled data pool is full of “invalid” data, such as the out-of-distribution data. To verify the function of the current AL methods in realistic scenarios, we build two datasets, named Bamboo-AL-CLS and Bamboo-AL-DET. The unlabeled data pool of these two datasets consists of both valid and invalid data.

From the experiments on these two dataset, we find that current AL methods lag in realistic scenarios. Specifically, those out-of-distribution (OOD) data extensively impedes the method effectiveness. Motivated by this limitation, we propose *OOD Rectification* to rectify the OOD data in the unlabeled pool, boosting the performance of AL methods.

### 6.3. Implementation Details

1) Upstream datasets. For image classification task, We build Bamboo-AL-CLS by randomly sampling 4K visual concepts from the BambooTX. Our active annotation pipeline is based on a 9.3M  $p_C^U$  (all crawled data of 4K concepts), giving 3.7M valid (labeled) images and 5.6M invalid

images.<sup>3</sup> For object detection task, we build Bamboo-AL-DET by selecting 80 concepts from the common concepts of BambooTX.

2) Sampling strategies. We explore two classical uncertainty sampling strategies, *i.e.* Entropy Sampling and Margin Sampling [63], and a state-of-the-art AL algorithm, ClusterMargin [17] that consider both the uncertainty and diversity. In addition, we study two representative methods for AL on detection tasks, namely the Entropy over Bounding Boxes and the Core-Set method [25, 29, 62]. The former method mainly considers the uncertainty in data, and the latter considers both uncertainty and diversity in data. Core-Set demonstrates satisfactory adaptability in realistic scenarios.

### 6.4. Results and Insights

**The Devils are in Uncertainty Modeling.** The number of  $s_C^L(1)$  (the first round valid data set of Bamboo-AL-CLS) retained in the first round AL batch  $s_C^U(1)$  are presented in Fig. 6 (a). Without OOD rectification (the current AL setting), all AL methods retain much less  $s_C^L(1)$  than random sampling (RS) in a given AL batch, namely much more invalid data. Specifically, Entropy Sampling that selects the largest valid data among other AL methods still selects 70% less data than RS, resulting in worse downstream performance. From our analysis, the uncertainty-based selecting strategy causes such inefficiency problems of AL methods. As discussed in [37], there are mainly two types of uncertainty for the deep models: *Aleatoric* and *Epistemic*. In particular, according to [20], the former is inconducive to model learning because such uncertainty implies invalid samples, mainly out-of-distribution data. The latter is uncertain to models yet is still in-distribution and informative, hence conducive to learning. Based on the unlabeled data pool in the realistic scenarios, a given AL batch would include the aleatoric uncertain samples, epistemic uncertain samples, and other samples. The last two are valid data for annotators, yet the first one is invalid data. Since uncertainty-based AL methods tend to select more uncertain data than RS, they include more aleatoric uncertain samples in their AL batch  $s_C^U$ . Eventually, annotators relatively retain few images in the final valid data set  $s_C^L$ . As shown in Fig. 6 (a), these AL methods’ performances are hence worse than RS.

**OOD Rec. Boosts AL Performance.** For a fixed size AL batch  $s_C^U$ , it has invalid aleatoric samples, valid and informative epistemic samples, and other valid yet less informative samples. OOD rectification filters out the OOD data that is closely related to the aleatoric uncertainty. Therefore, the reduced proportion of aleatoric samples implies more valid samples included in the  $s_C^U$ . Since AL methods include more

<sup>3</sup>In this section, we refer to  $p$  and  $s$  instead of  $\mathcal{P}$  and  $\mathcal{S}$  to indicate the image pool or image set in this simulated experiments.



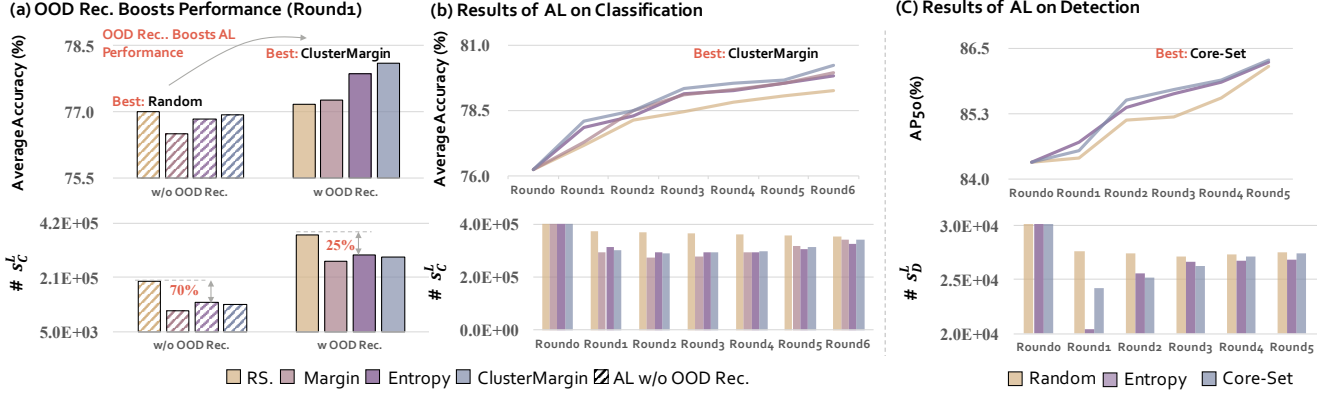


Figure 6. **The study of active annotation in Bamboo.** (a) current AL methods struggle in realistic scenarios. Random sampling achieves better performance than each AL method. *OOD Rectification* boosts all AL methods to outperform random sampling. With less valid data, AL methods are still more helpful for model training. It implies that the valid data that AL methods selected are much more informative. (b) and (c) in both classification and detection tasks, AL methods (ClusterMargin and Core-Set) that consider both the uncertainty and diversity, select the most valuable data for model training.  $s_C^L$  refers annotated valid data from a given AL batch. Average accuracy denotes the average performance of models on the downstream datasets.

Table 2. **Downstream classification tasks performance among different pre-training methods.** Bamboo achieves the state-of-the-arts linear probe performance on the downstream tasks. Lang. indicates image-text pair. Numbers in red are the performance gain on the same backbone network. Bamboo here refers to the Bamboo-CLS. Pets indicates OxfordPets. Flowers indicates OxfordFlower. Cars indicates StanfordCars. Aircraft indicates FGVC-Aircraft. IN1K indicates ImageNet1K. Results reported by the author are marked in gray. We mainly compare with the methods conducted on supervised learning. Other performance of current methods are also presented.

Method	Data	Annotation	Model	Paradigm	CIFAR10	CIFAR100	Food101	Pets	Flowers	SUN397	Cars	DTD	Caltech101	Aircraft	IN1K	AVG†
SwAV [10]	IN1K	1.2M	RN50	Self.	92.5	76.6	76.4	88.0	93.0	65.5	60.5	78.1	91.0	56.0	66.9	76.8
DINO [11]	IN1K	1.2M	RN50	Self.	93.7	79.2	77.2	89.2	96.2	66.0	68.3	77.6	92.3	63.1	83.3	79.8
SWSL [78]	IG-1B	1B	RN50	Semi.	94.7	79.5	79.1	94.4	94.6	67.8	65.9	77.8	96.1	58.4	81.2	80.9
WSL [48]	IG-1B	1B	RX101	Weak.	95.0	78.2	83.5	<b>95.5</b>	90.8	67.9	72.3	75.3	93.3	53.9	83.3	81.0
CLIP [55]	WIT	400M	RN50	Lang.	88.7	70.3	86.4	88.2	96.1	73.3	78.3	76.4	89.6	49.1	73.3	79.1
CLIP [55]	WIT	400M	B/16	Lang.	96.2	83.1	92.8	93.1	98.1	78.4	86.7	79.2	94.7	59.5	80.2	85.6
BiT [38]	IN1K	1.2M	RN50	Sup.	91.7	74.8	72.5	92.3	92.0	61.1	53.5	72.4	91.2	52.5	75.2	73.6
BiT [38]	IN22K	14M	RN50	Sup.	94.9	82.2	83.3	91.5	99.4	69.9	59.0	77.3	93.9	55.6	76.7	80.3
RN50	Bamboo	69M	RN50	Sup.	93.9	81.2	85.3	92.0	99.4	72.2	91.1	76.5	93.2	84.0	77.2	86.0 (+5.1)
B/16	Bamboo	69M	B/16	Sup.	<b>98.2</b>	<b>90.2</b>	<b>92.9</b>	95.1	<b>99.8</b>	<b>79.0</b>	<b>93.3</b>	<b>81.2</b>	<b>97.0</b>	<b>88.1</b>	<b>83.6</b>	<b>91.8 (+6.2)</b>

Table 3. **Comparisons of downstream detection tasks performance.** Pre-trained model on Bamboo achieves significant performance gain. Bamboo here refers to the Bamboo-DET. VOC means the PASCAL VOC dataset [21]. CITY. means the CityPersons dataset [86].

Method	Data	Anno.	Model	VOC AP50 ↑	CITY. MR ↓
FPN	COCO [64]	1M	RN50	85.1	16.2
FPN	OpenImages [64]	14M	RN50	82.4	16.8
FPN	Objects365	10M	RN50	86.4	14.7
FPN	Bamboo	27M	RN50	<b>87.5 (+1.1)</b>	<b>12.6 (+2.1)</b>

valid and informative epistemic samples than RS, they perform better after OOD rectification. As shown in Fig. 6 (a), with slightly less valid data, AL methods are still more helpful for model training, implying that their selected valid data is more informative.

**ClusterMargin and Core-Set are Better.** As shown in Fig. 6 (b,c), in both classification and detection tasks, AL methods (ClusterMargin and Core-Set) that consider both

the uncertainty and diversity select the most valuable data for model training.

## 6.5. Power of Bamboo as Pre-Training

**Information-Dense Annotations Matter.** As shown in Table 2, ResNet-50 (RN50) pre-trained on CLIP (400M) or IG-1B (1B) achieves better downstream task performance than BiT pre-trained on ImageNet1K (IN1K) [60]. However, compared to RN50 pre-trained on Bamboo, CLIP-RN50 or RN50 pre-trained on IG-1B achieves inferior performance. It indicates that the amount of informative-dense annotations instead of the sheer number of annotations is much more essential for model pre-training. Compared to CLIP that leverages the vast amount of image-text pairs on the web for pre-training, our Bamboo presents an active and continual framework that collect and annotate fully-supervised samples in a highly scalable manner.

**Comprehensive Label System (BambooTX) Helps.** As shown in Table 2, even though most methods pre-trained on IN1K, IG-1B, or WIT achieve more than 90% accuracy on the OxfordPets and OxfordFlower, they only achieve less than 80% accuracy on the StanfordCars and FGVC-Aircraft. It indicates that these pre-trained datasets might include more semantic concepts related to OxfordPets and OxfordFlower. Our BambooTX spreads a large spectrum of concepts. Particularly, it includes much more concepts that are neglected in the current public and nonpublic datasets. As a result, models pre-trained on Bamboo achieve much better performance than other methods. Beyond general object detection, it is also important to validate the generalization ability on the specific object detection problems like pedestrian detection.

**Bamboo is an Effective Pre-Training Source.** Compared to other methods, Bamboo achieves the best performance among downstream tasks on average. As shown in Table 2, ViT B/16 pretrained on Bamboo outperforms CLIP with 6.2 points gain. It indicates that our annotation is much more informative and hence more helpful for the model pre-training. In addition, Table 3 presents that ResNet-50 with FPN pretrained on Bamboo outperforms Objects365 with 1.1 points gain on PASCAL VOC and 2.1 points gain on CityPersons.

## 7. Conclusion

In our work, with a human-machine synergy, we actively and continually build a mega-scale and information-dense dataset, namely Bamboo. Bamboo is the largest clean image dataset available to the vision research community, in terms of the total number of images and the number of categories, for classification and detection tasks. Our key insight is that a unified and visually-oriented label system is crucial for model pre-training, and rectifying OOD samples is indispensable for AL to function in realistic scenarios. We have demonstrated the effectiveness of Bamboo as a better pre-training dataset for various downstream tasks and provided several valuable observations.

## References

- [1] The act partially amending the copyright act (act no.52 of 2021; enacted may, 2021), 2010. [17](#)
- [2] Andrei Barbu, David Mayo, Julian Alverio, William Luo, Christopher Wang, Danny Gutfreund, Joshua Tenenbaum, and Boris Katz. Objectnet: A large-scale bias-controlled dataset for pushing the limits of object recognition models. 2019. [16](#)
- [3] Josh Beal, Hao-Yu Wu, Dong Huk Park, Andrew Zhai, and Dmitry Kislyuk. Billion-scale pretraining with vision transformers for multi-task visual representations. *arXiv preprint arXiv:2108.05887*, 2021. [16](#)
- [4] Sara Beery, Arushi Agarwal, Elijah Cole, and Vighnesh Birodkar. The iwildcam 2021 competition dataset. *arXiv preprint arXiv:2105.03494*, 2021. [15](#)
- [5] Hoyt Ben. Duplicate image detection with perceptual hashing in python. <https://benhoyt.com/writings/duplicate-image-detection/#difference-hash-dhash>, 2017. [17](#)
- [6] Rishi Bommasani, Drew A Hudson, Ehsan Adeli, Russ Altman, Simran Arora, Sydney von Arx, Michael S Bernstein, Jeannette Bohg, Antoine Bosselut, Emma Brunskill, et al. On the opportunities and risks of foundation models. *arXiv preprint arXiv:2108.07258*, 2021. [2](#)
- [7] Lukas Bossard, Matthieu Guillaumin, and Luc Van Gool. Food-101 – mining discriminative components with random forests. In *ECCV*, 2014. [8](#)
- [8] Victoria Campbell. Authors guild v. google, inc. *DePaul J. Art Tech. & Intell. Prop. L*, 27:59, 2016. [17](#)
- [9] Mathilde Caron, Piotr Bojanowski, Armand Joulin, and Matthijs Douze. Deep clustering for unsupervised learning of visual features. In *ECCV*, pages 132–149, 2018. [3](#)
- [10] Mathilde Caron, Ishan Misra, Julien Mairal, Priya Goyal, Piotr Bojanowski, and Armand Joulin. Unsupervised learning of visual features by contrasting cluster assignments. *arXiv preprint arXiv:2006.09882*, 2020. [2](#), [3](#), [9](#)
- [11] Mathilde Caron, Hugo Touvron, Ishan Misra, Hervé Jégou, Julien Mairal, Piotr Bojanowski, and Armand Joulin. Emerging properties in self-supervised vision transformers. *arXiv preprint arXiv:2104.14294*, 2021. [9](#)
- [12] Soravit Changpinyo, Piyush Sharma, Nan Ding, and Radu Soricut. Conceptual 12M: Pushing web-scale image-text pre-training to recognize long-tail visual concepts. In *CVPR*, 2021. [17](#)
- [13] Ting Chen, Simon Kornblith, Mohammad Norouzi, and Geoffrey Hinton. A simple framework for contrastive learning of visual representations. In *ICML*, pages 1597–1607. PMLR, 2020. [3](#), [16](#)
- [14] Xinlei Chen, Haoqi Fan, Ross Girshick, and Kaiming He. Improved baselines with momentum contrastive learning. *arXiv preprint arXiv:2003.04297*, 2020. [2](#)
- [15] François Chollet. Xception: Deep learning with depthwise separable convolutions. In *CVPR*, pages 1251–1258, 2017. [3](#)
- [16] M. Cimpoi, S. Maji, I. Kokkinos, S. Mohamed, , and A. Vedaldi. Describing textures in the wild. In *CVPR*, 2014. [8](#)
- [17] Gui Citovsky, Giulia DeSalvo, Claudio Gentile, Lazaros Karydas, Anand Rajagopalan, Afshin Rostamizadeh, and Sanjiv Kumar. Batch active learning at scale. *arXiv preprint arXiv:2107.14263*, 2021. [2](#), [6](#), [8](#)
- [18] Jia Deng, Wei Dong, Richard Socher, Li-Jia Li, Kai Li, and Li Fei-Fei. Imagenet: A large-scale hierarchical image database. In *CVPR*, pages 248–255. Ieee, 2009. [2](#), [3](#), [6](#), [15](#)
- [19] Alexey Dosovitskiy, Philipp Fischer, Jost Tobias Springenberg, Martin Riedmiller, and Thomas Brox. Discriminative unsupervised feature learning with exemplar convolutional neural networks. *TPAMI*, 38(9):1734–1747, 2015. [3](#)
- [20] Daniel D’souza, Zach Nussbaum, Chirag Agarwal, and Sara Hooker. A tale of two long tails. *arXiv preprint arXiv:2107.13098*, 2021. [8](#)
- [21] Mark Everingham, Luc Van Gool, Christopher KI Williams, John Winn, and Andrew Zisserman. The pascal visual object classes (voc) challenge. *IJCV*, 88(2):303–338, 2010. [8](#), [9](#)
- [22] MS Fabian, Kasneci Gjergji, WEIKUM Gerhard, et al. Yago: A core of semantic knowledge unifying wordnet and wikipedia. In *WWW*, pages 697–706, 2007. [3](#)
- [23] Li Fei-Fei, Rob Fergus, and Pietro Perona. Learning generative visual models from few training examples: An incremental bayesian approach tested on 101 object categories. In *CVPR workshop*, pages 178–178. IEEE, 2004. [8](#)
- [24] Andrea Frome, German Cheung, Ahmad Abdulkader, Marco Zennaro, Bo Wu, Alessandro Bissacco, Hartwig Adam, Hartmut Neven, and Luc Vincent. Large-scale privacy protection in google street view. In *ICCV*, pages 2373–2380. IEEE, 2009. [17](#)
- [25] Yarin Gal. Uncertainty in deep learning. [3](#), [8](#)
- [26] Golnaz Ghiasi, Barret Zoph, Ekin D Cubuk, Quoc V Le, and Tsung-Yi Lin. Multi-task self-training for learning general representations. *arXiv preprint arXiv:2108.11353*, 2021. [2](#)
- [27] Ran Gilad-Bachrach, Amir Navot, and Naftali Tishby. Query by committee made real. *Advances in neural information processing systems*, 18, 2005. [3](#)
- [28] Ross Girshick. Fast r-cnn. *arXiv preprint arXiv:1504.08083*, 2015. [15](#)
- [29] Elmar Haussmann, Michele Fenzi, Kashyap Chitta, Jan Ivanec, Hanson Xu, Donna Roy, Akshita Mittel, Nicolas Koumchatzky, Clément Farabet, and Jose M. Alvarez. Scalable active learning for object detection. In *IEEE Intelligent Vehicles Symposium, IV 2020, Las Vegas, NV, USA, October 19 - November 13, 2020*, pages 1430–1435. IEEE, 2020. [8](#), [14](#), [15](#)
- [30] Kaiming He, Haoqi Fan, Yuxin Wu, Saining Xie, and Ross Girshick. Momentum contrast for unsupervised visual representation learning. In *CVPR*, pages 9729–9738, 2020. [2](#), [3](#), [4](#), [8](#)
- [31] Kaiming He, Xiangyu Zhang, Shaoqing Ren, and Jian Sun. Deep residual learning for image recognition. In *CVPR*, pages 770–778, 2016. [3](#)
- [32] Matthew Honnibal and Ines Montani. spaCy 2: Natural language understanding with Bloom embeddings, convolutional neural networks and incremental parsing. To appear, 2017. [3](#), [4](#)

- [33] Siyu Huang, Tianyang Wang, Haoyi Xiong, Jun Huan, and Dejing Dou. Semi-supervised active learning with temporal output discrepancy. In *ICCV*, pages 3447–3456, 2021. 8
- [34] Juan Eugenio Iglesias, Ender Konukoglu, Albert Montillo, Zhuowen Tu, and Antonio Criminisi. Combining generative and discriminative models for semantic segmentation of ct scans via active learning. In *Biennial International Conference on Information Processing in Medical Imaging*, pages 25–36. Springer, 2011. 3
- [35] Ajay J Joshi, Fatih Porikli, and Nikolaos Papanikolopoulos. Multi-class active learning for image classification. In *CVPR*, pages 2372–2379. IEEE, 2009. 3
- [36] Parneet Kaur, Karan Sikka, Weijun Wang, Serge Belongie, and Ajay Divakaran. Foodx-251: A dataset for fine-grained food classification. *arXiv preprint arXiv:1907.06167*, 2019. 15
- [37] Alex Kendall and Yarin Gal. What uncertainties do we need in bayesian deep learning for computer vision? *arXiv preprint arXiv:1703.04977*, 2017. 8
- [38] Alexander Kolesnikov, Lucas Beyer, Xiaohua Zhai, Joan Puigcerver, Jessica Yung, Sylvain Gelly, and Neil Houlsby. Big transfer (bit): General visual representation learning. In *ECCV*, pages 491–507. Springer, 2020. 2, 9, 16
- [39] Simon Kornblith, Jonathon Shlens, and Quoc V Le. Do better imagenet models transfer better? In *CVPR*, pages 2661–2671, 2019. 4, 8
- [40] Jonathan Krause, Michael Stark, Jia Deng, and Li Fei-Fei. 3d object representations for fine-grained categorization. In *4th International IEEE Workshop on 3D Representation and Recognition (3dRR-13)*, Sydney, Australia, 2013. 3, 8
- [41] Alex Krizhevsky, Geoffrey Hinton, et al. Learning multiple layers of features from tiny images. 2009. 2, 3, 8
- [42] Alina Kuznetsova, Hassan Rom, Neil Alldrin, Jasper Uijlings, Ivan Krasin, Jordi Pont-Tuset, Shahab Kamali, Stefan Popov, Matteo Mallocci, Alexander Kolesnikov, et al. The open images dataset v4. *IJCV*, 128(7):1956–1981, 2020. 2, 3, 6, 7, 15
- [43] Gustav Larsson, Michael Maire, and Gregory Shakhnarovich. Learning representations for automatic colorization. In *ECCV*, pages 577–593. Springer, 2016. 3
- [44] Junnan Li, Pan Zhou, Caiming Xiong, Richard Socher, and Steven CH Hoi. Prototypical contrastive learning of unsupervised representations. *arXiv preprint arXiv:2005.04966*, 2020. 3
- [45] Tsung-Yi Lin, Piotr Dollár, Ross Girshick, Kaiming He, Bharath Hariharan, and Serge Belongie. Feature pyramid networks for object detection. In *CVPR*, pages 2117–2125, 2017. 15
- [46] Tsung-Yi Lin, Michael Maire, Serge Belongie, James Hays, Pietro Perona, Deva Ramanan, Piotr Dollár, and C Lawrence Zitnick. Microsoft coco: Common objects in context. In *ECCV*, pages 740–755. Springer, 2014. 2, 3, 4, 6, 15, 17
- [47] Ilya Loshchilov and Frank Hutter. Decoupled weight decay regularization. *arXiv preprint arXiv:1711.05101*, 2017. 15
- [48] Dhruv Mahajan, Ross Girshick, Vignesh Ramanathan, Kaiming He, Manohar Paluri, Yixuan Li, Ashwin Bharambe, and Laurens Van Der Maaten. Exploring the limits of weakly supervised pretraining. In *ECCV*, pages 181–196, 2018. 3, 9
- [49] S. Maji, J. Kannala, E. Rahtu, M. Blaschko, and A. Vedaldi. Fine-grained visual classification of aircraft. Technical report, 2013. 8
- [50] George A Miller. *WordNet: An electronic lexical database*. MIT press, 1998. 2, 3
- [51] Ishan Misra and Laurens van der Maaten. Self-supervised learning of pretext-invariant representations. In *CVPR*, pages 6707–6717, 2020. 3
- [52] M-E Nilsback and Andrew Zisserman. A visual vocabulary for flower classification. In *CVPR*, volume 2, pages 1447–1454. IEEE, 2006. 3, 8
- [53] Omkar M Parkhi, Andrea Vedaldi, Andrew Zisserman, and CV Jawahar. Cats and dogs. In *CVPR*, pages 3498–3505. IEEE, 2012. 3, 8
- [54] Lukáš Pícek, Milan Šulc, Jiří Matas, Jacob Heilmann-Clausen, Thomas S Jeppesen, Thomas Læssøe, and Tobias Frøslev. Danish fungi 2020—not just another image recognition dataset. *arXiv preprint arXiv:2103.10107*, 2021. 15
- [55] Alec Radford, Jong Wook Kim, Chris Hallacy, Aditya Ramesh, Gabriel Goh, Sandhini Agarwal, Girish Sastry, Amanda Askell, Pamela Mishkin, Jack Clark, et al. Learning transferable visual models from natural language supervision. *arXiv preprint arXiv:2103.00020*, 2021. 2, 3, 9, 16, 17
- [56] Anant Ram, Jalal Sunita, Anand Jalal, and Kumar Manoj. A density based algorithm for discovering density varied clusters in large spatial databases. *International Journal of Computer Applications*, 3, 06 2010. 14
- [57] Pengzhen Ren, Yun Xiao, Xiaojun Chang, Po-Yao Huang, Zhihui Li, Xiaojiang Chen, and Xin Wang. A survey of deep active learning. *arXiv preprint arXiv:2009.00236*, 2020. 2
- [58] Shaoqing Ren, Kaiming He, Ross Girshick, and Jian Sun. Faster r-cnn: Towards real-time object detection with region proposal networks. *arXiv preprint arXiv:1506.01497*, 2015. 15
- [59] Dan Roth and Kevin Small. Margin-based active learning for structured output spaces. In *European Conference on Machine Learning*, pages 413–424. Springer, 2006. 14
- [60] Olga Russakovsky, Jia Deng, Hao Su, Jonathan Krause, Sanjeev Satheesh, Sean Ma, Zhiheng Huang, Andrej Karpathy, Aditya Khosla, Michael Bernstein, et al. Imagenet large scale visual recognition challenge. *IJCV*, 115(3):211–252, 2015. 8, 9
- [61] Christoph Schuhmann, Richard Vencu, Romain Beaumont, Robert Kaczmarczyk, Clayton Mullis, Aarush Katta, Theo Coombes, Jenia Jitsev, and Aran Komatsuzaki. Laion-400m: Open dataset of clip-filtered 400 million image-text pairs, 2021. 17
- [62] Ozan Sener and Silvio Savarese. Active learning for convolutional neural networks: A core-set approach. In *ICLR*. OpenReview.net, 2018. 6, 8, 15
- [63] Burr Settles. Active learning literature survey. 2009. 2, 3, 8
- [64] Shuai Shao, Zeming Li, Tianyuan Zhang, Chao Peng, Gang Yu, Xiangyu Zhang, Jing Li, and Jian Sun. Objects365: A large-scale, high-quality dataset for object detection. In *ICCV*, pages 8430–8439, 2019. 2, 6, 9, 14, 15, 17



- [65] Baris Sumengen, Anand Rajagopalan, Gui Citovsky, David Simcha, Olivier Bachem, Pradipta Mitra, Sam Blasiak, Mason Liang, and Sanjiv Kumar. Scaling hierarchical agglomerative clustering to billion-sized datasets, 2021. [14](#)
- [66] Chen Sun, Abhinav Shrivastava, Saurabh Singh, and Abhinav Gupta. Revisiting unreasonable effectiveness of data in deep learning era. In *ICCV*, pages 843–852, 2017. [2](#), [3](#)
- [67] Raphael Sznitman and Bruno Jedynak. Active testing for face detection and localization. *TPAMI*, 32(10):1914–1920, 2010. [3](#)
- [68] Thomas Pellissier Tanon, Gerhard Weikum, and Fabian M. Suchanek. Yago 4: A reason-able knowledge base. *The Semantic Web*, 12123:583 – 596, 2020. [3](#)
- [69] Bart Thomee, David A Shamma, Gerald Friedland, Benjamin Elizalde, Karl Ni, Douglas Poland, Damian Borth, and Li-Jia Li. Yfcc100m: The new data in multimedia research. *Communications of the ACM*, 59(2):64–73, 2016. [6](#)
- [70] Simon Tong and Daphne Koller. Support vector machine active learning with applications to text classification. *Journal of machine learning research*, 2(Nov):45–66, 2001. [3](#)
- [71] Grant Van Horn, Oisin Mac Aodha, Yang Song, Yin Cui, Chen Sun, Alex Shepard, Hartwig Adam, Pietro Perona, and Serge Belongie. The inaturalist species classification and detection dataset. In *CVPR*, pages 8769–8778, 2018. [3](#), [15](#)
- [72] Alexander Vezhnevets, Vittorio Ferrari, and Joachim M Buhmann. Weakly supervised structured output learning for semantic segmentation. In *CVPR*, pages 845–852. IEEE, 2012. [3](#)
- [73] Denny Vrandečić and Markus Krötzsch. Wikidata: a free collaborative knowledgebase. *Communications of the ACM*, 57(10):78–85, 2014. [2](#), [3](#)
- [74] Dan Wang and Yi Shang. A new active labeling method for deep learning. In *IJCNN*, pages 112–119, 2014. [14](#)
- [75] Zhirong Wu, Yuanjun Xiong, Stella X Yu, and Dahua Lin. Unsupervised feature learning via non-parametric instance discrimination. In *CVPR*, pages 3733–3742, 2018. [3](#)
- [76] Jianxiong Xiao, Krista A Ehinger, James Hays, Antonio Torralba, and Aude Oliva. Sun database: Exploring a large collection of scene categories. *IJCV*, 119(1):3–22, 2016. [3](#), [8](#)
- [77] Qizhe Xie, Minh-Thang Luong, Eduard Hovy, and Quoc V Le. Self-training with noisy student improves imagenet classification. In *CVPR*, pages 10687–10698, 2020. [3](#)
- [78] I Zeki Yalniz, Hervé Jégou, Kan Chen, Manohar Paluri, and Dhruv Mahajan. Billion-scale semi-supervised learning for image classification. *arXiv preprint arXiv:1905.00546*, 2019. [2](#), [3](#), [9](#)
- [79] Jingkang Yang, Kaiyang Zhou, Yixuan Li, and Ziwei Liu. Generalized out-of-distribution detection: A survey. *arXiv preprint arXiv:2110.11334*, 2021. [5](#)
- [80] Kaiyu Yang, Klint Qinami, Li Fei-Fei, Jia Deng, and Olga Russakovsky. Towards fairer datasets: Filtering and balancing the distribution of the people subtree in the imagenet hierarchy. In *Proceedings of the 2020 Conference on Fairness, Accountability, and Transparency*, pages 547–558, 2020. [4](#)
- [81] Kaiyu Yang, Jacqueline Yau, Li Fei-Fei, Jia Deng, and Olga Russakovsky. A study of face obfuscation in imagenet. *arXiv preprint arXiv:2103.06191*, 2021. [17](#)
- [82] Linjie Yang, Ping Luo, Chen Change Loy, and Xiaoou Tang. A large-scale car dataset for fine-grained categorization and verification. In *ICCV*, pages 3973–3981, 2015. [15](#)
- [83] Yi Yang, Zhigang Ma, Feiping Nie, Xiaojun Chang, and Alexander G Hauptmann. Multi-class active learning by uncertainty sampling with diversity maximization. *IJCV*, 113(2):113–127, 2015. [3](#)
- [84] Xiaohua Zhai, Joan Puigcerver, Alexander Kolesnikov, Pierre Ruysen, Carlos Riquelme, Mario Lucic, Josip Djolonga, Andre Susano Pinto, Maxim Neumann, Alexey Dosovitskiy, et al. A large-scale study of representation learning with the visual task adaptation benchmark. *arXiv preprint arXiv:1910.04867*, 2019. [4](#), [8](#)
- [85] Richard Zhang, Phillip Isola, and Alexei A Efros. Colorful image colorization. In *ECCV*, pages 649–666. Springer, 2016. [3](#)
- [86] Shanshan Zhang, Rodrigo Benenson, and Bernt Schiele. Citypersons: A diverse dataset for pedestrian detection. In *CVPR*, July 2017. [2](#), [8](#), [9](#)
- [87] Bolei Zhou, Agata Lapedriza, Aditya Khosla, Aude Oliva, and Antonio Torralba. Places: A 10 million image database for scene recognition. *TPAMI*, 2017. [3](#), [15](#)
- [88] Barret Zoph, Golnaz Ghiasi, Tsung-Yi Lin, Yin Cui, Hanxiao Liu, Ekin D Cubuk, and Quoc V Le. Rethinking pre-training and self-training. *arXiv preprint arXiv:2006.06882*, 2020. [3](#)
- [89] Ding-Nan Zou, Song-Hai Zhang, Tai-Jiang Mu, and Min Zhang. A new dataset of dog breed images and a benchmark for fine-grained classification. *Computational Visual Media*, 2020. [15](#)

## A. About Bamboo

We briefly introduce why we name our dataset as *Bamboo*. Firstly, in addition to Antarctica and the European continent, bamboo can be found on all continents. *Bamboo* is comprehensive, the scale of both the label system and the annotated data is the largest among all the publicly available datasets. Secondly, conciseness is a critical characteristic of bamboo in eastern culture. *Bamboo* is information-dense. The label system is constructed by a thorough integration of public datasets and knowledge bases. Its label system and the annotated data are designed to guarantee both coverage and informativeness. Our active annotation pipeline specifically selects the annotated data to reduce model uncertainty. Thirdly, bamboo is the fastest growing plant in the world. Our label system enables the dataset to keep on growing with the proposed automatic concept linking strategies. We can constantly absorb new categories in the real world and integrate them into our label system. Moreover, by leveraging the ever-increasing internet data, our active annotation pipeline will steadily expand the size of *Bamboo* in a sustainable manner.

## B. Experiments

### B.1. The Influence Of Similar Semantic Proposals

For the object detection task, the total annotation cost depends on the number of proposals. Images with dense proposals are more expensive than sparse ones. Many proposals with similar semantics tend to form a group in a single image based on our observation. To evaluate their effectiveness, we conduct the following experiments on Objects365 [64] dataset.

Firstly, we define an image as a crowded image if it contains at least one category with more than 15 proposals. By removing all 27K crowded images from the full Objects365 dataset, we denote the remaining part as Objects365-sparse. Keeping the number of proposals the same as Objects365-sparse, we randomly removed 90K images from the full Objects365 dataset and marked the remaining part as Objects365-random. Furthermore, keeping the total object amount the same as Objects365-sparse, we randomly removed 101K non-crowded images from the full Objects365 dataset and denoted the remaining part as Objects365-dense.

Dataset	Images	Proposals	VOC AP50 $\uparrow$
Objects365-sparse	581K	8.2M	86.3
Objects365-random	519K	8.2M	85.8
Objects365-dense	508K	8.2M	85.1

As shown above, given the same annotation budget, we find that choosing to label non-crowded images yields better results for pre-training performance. Therefore, as men-

tioned in Sec. 3.3.2 of the main paper, we filter out covariate shift data in the OOD rectification step.

### B.2. Studies on Active Annotation

#### B.2.1 Methods

**Image Classification.** *Random Sampling* serves as a comparison baseline to prove the benefit of active learning algorithms, which selects  $k$  examples from at random.

*Uncertainty Sampling (Entropy and Margin)* selects  $k$  examples from  $p_C^R(r)$ <sup>4</sup> according to the maximum uncertainty based on the model’s prediction and different measures. Entropy Sampling takes the entropy of the example’s predictive probability distribution as a measure of uncertainty, defined as  $H((f(x; \theta)_y)_{y=1}^K)$ , where  $f(x; \theta)_y$  is the predictive probability of class  $y$  and  $H(p) = -\sum_{i=1}^K p_i \ln \frac{1}{p_i}$  [74]. While Margin Sampling calculates the difference between the largest two probabilities of predicted class, defined as  $f(x; \theta)_{\hat{y}_1} - f(x; \theta)_{\hat{y}_2}$ , where  $\hat{y}_1$  and  $\hat{y}_2$  are respectively the first and second most probable predicted class labels [59].

*ClusterMargin\** uses information from both the model and the unlabeled pool, which combines notions of uncertainty and diversity at large scales. Drawing on this idea, we reproduce ClusterMargin\*. Unlike the original paper that runs once Hierarchical Agglomerative Clustering (HAC) [65] on the embeddings of all examples in the entire unlabeled pool as an initial step at the beginning, we first use Margin Sampling to select  $k_m$  examples with lowest margin scores (highest margin uncertainty). Then we cluster them according to the embeddings from the penultimate layer using Density-Based Spatial Clustering of Applications with Noise (DBSCAN) [56] and finally employ a round-robin sampling scheme to sample  $k_t$  ( $k_m > k_t$ , we set  $k_m = 2 * k_t$  in the simulating experiments) examples orderly in each AL round for ensuring more uncertainty, diversity, and simplicity.

**Object Detection.** *Random Sampling* also serves as a comparison baseline for active learning in the object detection context, similarly to the image classification context.

*Entropy over Bounding Boxes (DET-ENT)* considers the aggregation of bounding-box-wise detector entropy. Following [29], for each bounding box within an image, we leverage the predicted probability  $p_c$  at ground-truth class  $c$  as the Bernoulli random variable to compute the entropy of this bounding box as  $H(p_c) = p_c \log p_c + (1 - p_c) \log (1 - p_c)$ . Then, with the aggregation method of taking the average of entropy over all bounding boxes in one image, we get the single score to evaluate the uncertainty of this image.

<sup>4</sup>If not mentioned otherwise,  $p(r)$  denotes the data pool at round  $r$  and  $s(r)$  denotes the selected data set at round  $r$ . The upper index  $L$  stands for labeled, upper index  $R$  stands for rectified data, and upper index  $U$  stands for unlabelled. The lower index  $C$  means classification and  $D$  means detection.

*Core-set* takes into consideration not only the uncertainty of a single image, but also the distance of embeddings towards other labeled images. Following the greedy implementation [29] of the initially proposed core-set approach [62] for active learning, we choose images from the unlabeled set with the largest weighted distance towards the labeled set by  $\arg \max_{x_u \in s_C^U(r)} \min_{x_l \in p_D^L(r-1)} H(x_u) \text{dist}(x_u, x_l)$ , where  $H(\cdot)$  denotes the uncertainty measurement as mentioned above and  $\text{dist}(\cdot)$  calculates the cosine similarity of the reshaped feature map in the last layer of the backbone.

### B.2.2 Experimental Setup

**Image Classification.** The initial training set  $p_C^L(0)$  of Bamboo-AL-CLS has 2M images. Our active learning batches  $s_C^U$  for simulated experiments is 0.5M. This number of AL batch is 10% of the actual AL batch in our realistic active annotation pipeline. Since ClusterMargin\* includes a step to cluster feature embedding (penultimate layer of the model), we train a ResNet-50 model inserted with a fully-connected hidden layer of 128 dimensions before the final classification head. Otherwise, the penultimate layer (2048) of the original ResNet-50 is too large to conduct clustering. Besides, we adopt the model reset training strategy instead of finetuning the model from the previous rounds for all AL rounds and methods, employing an AdamW [47] optimizer of 30 epochs using a cosine decay scheduler with two epochs of linear warm-up and 2,048 batch size. The backbone is initialized from the pre-trained model officially offered by PyTorch. The initial learning rate, weight decay, and warm-up learning rate are  $2 \times 10^{-8}$ ,  $10^{-6}$ , and  $2 \times 10^{-2}$ .

Besides the shared initial training step, we run six rounds each in all AL methods, including Random Sampling, Entropy, Margin, and ClusterMargin\*. Following the active learning loop, we get a batch of images:  $s_C^U$  selected by the methods mentioned above. In each round  $r$ , we take the intersection of  $s_C^U(r)$  and the valid 3.7M labeled images, forming the valid image  $s_C^U(r)$ . At the end of each round, we remove  $s_C^U(r)$  from  $p_C^U(r-1)$  and add  $s_C^U(r)$  into  $s_C^U(r-1)$  to form the new labeled pool  $s_C^U(r)$ , on which we train a new model  $\phi(r)$  and report its downstream performance.

**Object Detection.** Bamboo-AL-DET is constructed by selecting 80 concepts from the common concepts of the BambooTX. Similar to the construction of Bamboo-AL-CLS, Bamboo-AL-DET finally has a 490K unlabelled image pool  $p_D^U$  which includes 321K valid images. The initial training set  $p_D^L(0)$  has 168K images.

We conducted experiments on the Resnet50 based FPN [45] backbone, with the learning rate of 0.015 on 32 V100 GPUs, total batch size of 256, SGD optimizer of momentum 0.9 and weight decay of 0.0001, MultiStep learning rate scheduler of 26 epochs, and learning rate decay on 16, 22 epochs by decay rate of 0.1. We also applied  $L_2$  type

gradient clip with the maximum norm of 5.0. For detectors, we leveraged the Faster-RCNN [58] model with Cross-Entropy-Loss for classification and Smoothed-L1-Loss [28] for bounding box regression.

For each round  $r$ , we use this model trained on  $p_D^L(r-1)$  to score the randomly selected 100K candidate images from the last round unlabeled set  $p_D^U(r-1)$  and then choose the top 50K images by each AL method, respectively. Similar to the experiments in image classification, we filter out invalid images during annotation. Then, we add the newly annotated images to the training set and train a new model from scratch to replace the current model. We iterative repeat the above pipeline for the following AL rounds, expand the training set and update the trained model.

### B.3. Power of Bamboo as Pre-Training

#### B.3.1 Experimental Setup

**Training.** We train the models on 64 A100 GPUs for image classification, with a total batch size of 8,192. We employ an AdamW [47] optimizer of 30 epochs using a cosine decay scheduler with two epochs of linear warm-up. The ResNet-50 backbone is initialized from the model officially offered by PyTorch. The ViT B/16 backbone is initialized from model pre-trained on ImageNet1K provided by timm.<sup>5</sup> The weight decay, and warm-up learning rate are  $2 \times 10^{-8}$ ,  $10^{-6}$ , and  $2 \times 10^{-2}$ . Besides the new annotated data, we include ImageNet22K [18], INaturalist2021 [71], Herbarium2021,<sup>6</sup> Danish Fungi 2020 [54], iWildCam2020 [4], TsinghuaDogs [89], Places [87], FoodX-251 [36], CompCars [82] in the upstream classification dataset training. We train the models on 48 A100 GPUs for detection, with a total batch size of 384, a total learning rate of 0.4, SGD optimizer of momentum 0.9, and a weight decay of 0.0001. We use the MultiStep learning rate scheduler with the decay rate of 0.1 on [16, 22] epochs and train for 26 epochs in total. We also applied warm-up learning rate of 0.0004 for 1 epoch. Similar to our studies on active annotation as mentioned in Sec. B.2, we used Cross-Entropy-Loss for categorization and Smoothed-L1-Loss for bounding box regression. Besides the new annotated data, we include COCO [46], Objects365 [64] and OpenImages [42] in the upstream object detection dataset training.

**Evaluation.** For classification, we train a logistic regression classifier for the linear probe evaluation setting. We finetune the model on 8 1080-Ti GPUs for detection, with the batch size of 16, SGD optimizer of momentum 0.9, and weight decay 0.0001 by loading the weights of backbone and FPN. We conduct a grid search on learning rate among  $[5 \times 10^{-4}, 1 \times 10^{-3}, 5 \times 10^{-3}, 1 \times 10^{-2}]$ . The learning rate is decayed by 0.1 at 16 and 18 and stopped training at 19 epochs.

<sup>5</sup><https://github.com/rwightman/pytorch-image-models/tree/master/timm>

<sup>6</sup><https://www.kaggle.com/c/herbarium-2021-fgvc8/overview>

Table 4. **Comparisons of zero-shot downstream classification tasks performance among different pre-training methods.** Bamboo achieves the state-of-the-arts linear probe performance on the downstream tasks. Lang. indicates image-text pair. Numbers in **red** are the performance gain on the same backbone network. Bamboo here refers to the Bamboo-CLS. Pets indicates OxfordPets. Flowers indicates OxfordFlower. Cars indicates StanfordCars. Aircraft indicates FGVC-Aircraft. IN1K indicates ImageNet1K. Results reported by the author are marked in gray. We mainly compare with the methods conducted on supervised learning. Other performance of current methods are also presented.

Method	Data	Annotation	Model	Paradigm	CIFAR10	CIFAR100	Food101	Pets	Flowers	SUN397	Cars	DTD	Caltech101	Aircraft	IN1K	AVG↑
CLIP [55]	WIT	400M	R50	Lang.	91.6	68.7	89.2	88.9	70.4	65.2	65.6	46	89.3	27.1	68.6	70.0
RN50	Bamboo	49M	RN50	Sup.	93.8	67.7	81.6	74.3	87.3	58.7	63.0	51.1	88.4	87.2	82.5	76.0 (+6.0)

Table 5. **Comparisons of fine-tuning downstream classification tasks performance among different pre-training methods.** Bamboo achieves the state-of-the-arts fine-tuning performance on the downstream tasks.

Method	Data	Annotation	Model	Paradigm	CIFAR10	CIFAR100	Food101	Pets	Flowers	SUN397	Cars	DTD	Caltech101	Aircraft	IN1K	AVG↑
DINO	IN1K	1.2M	RN50	Self.	97.1	84.0	86.3	90.0	96.1	65.2	84.6	77.6	91.4	81.8	66.5	83.7
SWAV	IN1K	1.2M	RN50	Self.	97.2	84.2	86.0	90.3	95.7	64.4	83.9	77.2	91.7	81.2	66.9	83.5
SWSL	IG-1B	1B	RN50	Semi.	97.0	86.5	87.3	94.4	97.0	66.0	88.5	78.3	93.8	84.0	81.7	86.8
BiT-S	IN1K	1.2M	RN50	Sup.	97.0	85.0	85.7	92.8	95.0	60.3	87.5	74.7	92.0	83.8	75.2	84.5
BiT-M	IN22K	14M	RN50	Sup.	97.6	86.2	87.9	91.5	98.1	64.2	88.2	78.4	92.9	84.3	76.7	86.0
RN50	Bamboo	49M	RN50	Sup.	97.3	87.0	87.5	92.0	99.4	72.2	91.4	77.1	93.9	85.9	77.1	87.3 (+0.5)

### B.3.2 Finetuning Transfer

We compared our model pre-trained on Bamboo to various with the ResNet-50 backbone. We present the fine-tuning transfer performance of the models pre-trained on Bamboo. The finetuning strategy among each downstream task is followed by the SimCLR [13]. Table 5 shows the comparison. Bamboo model achieves a 1.3% average accuracy gain compared to BiT-M pre-trained on the current largest public classification dataset: ImageNet22K. It indicates a larger, carefully annotated dataset can continually improve the performance of models. Besides, Bamboo model achieves a 0.5% average accuracy gain compared to SWSL, pre-trained on the IG-1B with 1B weakly supervised hashtags. Bamboo is 20 times smaller than IG-1B, which indicates that the amount of informative-dense annotations instead of the sheer number of weak annotations is much more essential for model pre-training.

### B.3.3 Zero-Shot Transfer

We present the zero-shot transfer performance of the models pre-trained on Bamboo. We compared our model pre-trained on Bamboo to CLIP models with the same backbone.

Table 4 shows the comparison. From the table, it can be seen that Bamboo model conclusively outperforms CLIP model with the same backbone: ViT B/16. Specifically, Bamboo model achieves a 6% average accuracy gain. On the FGVC-Aircraft, Bamboo model achieves 87.2%, despite having never seen any training images from this dataset. Bamboo includes all the concepts in the down-

stream tasks. However, we conduct data overlap analysis of Bamboo in Sec. C, ensuring Bamboo rarely includes downstream data.

### B.3.4 Robustness to Natural Distribution Shift

We conduct experiments on the ObjectNet [2] to compare Bamboo models with other models when evaluated on the data with controls for rotation, background, and viewpoint. ObjectNet is a dataset collected in the real world, where multiple objects are present most of the time. There are 313 object classes in total, with 113 overlapping with ImageNet1K. We follow the literature [38, 55] and evaluate our models on those 113 classes.

Method	Data	Model	Para.	ObjectNet ↑
BiT-L [38]	JFT-300M	R50	Weak.	37.6
ANN-1.3B [3]	ANN-1.3B	B/16	Weak.	50.7
R50	Bamboo	R50	Sup.	<b>38.8 (+1.2)</b>
B/16	Bamboo	B/16	Sup.	<b>53.9 (+3.2)</b>

As shown above, we compare Bamboo models with the state-of-the-art model with the same backbone. Specifically, ResNet-50 pre-trained on Bamboo achieves 1.2% gains compared with ResNet-50 pre-trained on JFT-300M. ViT B/16 pre-trained on Bamboo achieves 3.2% gains compared with ViT B/16 pre-trained on Anno-1.3B. Note that even though JFT-300M and Anno-1.3B are much larger than Bamboo, the informative data in Bamboo is more helpful for pre-trained models in real scenarios.



### B.3.5 Pre-Training Performance of Bamboo

Besides the downstream tasks in the main paper, we further introduce COCO [46] dataset. Compared to pre-training on other datasets, Bamboo achieves the best performance.

Method	Data	Anno.	Model	COCO
FPN	OpenImages [64]	14M	RN50	37.4
FPN	Objects365	10M	RN50	39.3
FPN	Bamboo	27M	RN50	<b>43.9 (+4.6)</b>

As shown above, ResNet-50 with FPN pre-trained on Bamboo outperforms Objects365 with 4.4 points gain.

## C. Social Impact

The proposed Bamboo dataset and pre-training model shows the capacity and generalization of learned image representation which could benefit many applications of computer vision. However, the usage of our data might bring several risks, such as data overlapping, privacy, and problematic content. We discuss these risks and their mitigation strategies as follows.

**Data Overlapping.** A concern with pre-training on a very large dataset is unintentional overlap with downstream evaluation [55]. To enable a meaningful test of generalization, we identify and remove all duplicates among upstream data. Specifically, we utilize Difference Hash (DHash) [5] to present the information of each image. We calculate the hash-code of each downstream image and each crawled image. Two images with the same hash-code are regarded as similar ones. Then, we filter out the crawled images that are similar to downstream images. Based on the above method, we discard 122,939 images for classification and 1,046 images for detection from the unlabeled pool.

**Copyright.** We crawl only the data under the Creative Commons license (CC-BY) for the Bamboo-DET. This license allows free use, redistribution, and adaptation for non-commercial purposes. For the Bamboo-CLS data, 30% of data is under the CC-BY license because of its large volume of data. For Bamboo-CLS data that is not under the CC-BY license, referred to LAION-400M [61] and Conceptual 12M [12], we only present the lists of URLs to this data without redistribution. We build the meta file as follow.

[image\_url] [class\_index]

Referred to *Authors Guild, Inc. v. Google Inc.* [8], training data on the copyrighted works might be considered as transformative uses and was thus might be regarded as *Fair Use*<sup>7</sup>. In addition, referred to *Article 30-4 of the new Copyright Act* [1], there are no restrictions on the subject, purpose, and method of data analysis, and there is no obligation to compensate the copyright holder. However, we admit

<sup>7</sup><https://www.copyright.gov/fair-use/index.html>

that using a copyright material as training data is still a controversial issue in Artificial Intelligence, and we would no doubt follow the newest law worldwide. Bamboo is specifically open for non-commercial research and/or educational purposes to respect the copyright law. For researchers and educators who wish to use copyrighted images for that purpose, training or benchmarking models with copyrighted works would be qualified as *transformative* uses and thus not infringe copyright law in the U.S.<sup>7</sup>. Nevertheless, the users must strictly follow the Flickr Terms of Use.<sup>8</sup> And the users of these images accept full responsibility for the use of the image.

**Problematic Content.** The problematic contents such as drugs, nudity, and other offensive content exist in the web data. As mentioned in main paper, the annotators were asked to discard such images instead of conducting annotation.

**Privacy.** To mitigate privacy issues with public visual datasets, researchers have attempted to obfuscate private information before publishing the data [24, 81]. We plan to follow this line of work to blur faces, license plates in our new annotated data. In addition, if the original picture found at the URL present on the Bamboo on the record states users' names, phone numbers, or any personal information, users can request a takedown of this image.

**Bias.** The images were crawled from Flickr thus inheriting all the biases of that website. The usage of user generated data might bring the risk of bias. We plan to tackle this problem by balancing various categories.

<sup>8</sup><https://www.flickr.com/help/terms/api>